Available online at www.sciencedirect.com
SCIENCE DIRECT®

Journal of the European Ceramic Society 24 (2004) 2187–2192
www.elsevier.com/locate/jeurceramsoc

Lifetime prediction for mechanically stressed low temperature co-fired ceramics

Henning Dannheim[a], Ulrich Schmid[b], Andreas Roosen[a,*]

[a]*University of Erlangen-Nuremberg, Institute of Materials Science, Glass and Ceramics, Martensstr. 5, 91058 Erlangen, Germany*
[b]*EADS Deutschland GmbH, Department SC/IRT/LG-ME, 81663 München, Germany*

Received 8 January 2003; received in revised form 22 July 2003; accepted 29 July 2003

Abstract

Multilayer ceramics based on LTCC (low temperature co-fired ceramics) are gaining increasing interest in the manufacturing of high-integrated devices for microelectronic applications. In many applications the parts are exposed to mechanical stresses, which is an important issue regarding the reliability of the device. To predict the life time of LTCC multilayer devices, and to extend the application range of LTCC, basic mechanical data of this material are needed. In this paper sintered LTCC laminates are investigated concerning their flexural strength, crack growth rate, and life time prediction. The flexural inert strength of the investigated LTCC material is about 450 MPa. In applications with a stress level of 100 MPa, like mass flow sensors for the measurement of injected fuel quantities, acceptable lifetimes are achieved. This means that LTCC is an interesting material to fabricate devices, in which LTCC fulfils the requirements of a functional and structural material.

Keywords: failure analysis; lifetime; LTCC; mechanical properties; sensors; substrates

1. Introduction

Multilayer ceramics based on LTCC (low temperature co-fired ceramics) are gaining increasing interest in the manufacturing of high-integrated devices for microelectronic applications. Compared to the HTCC (high temperature co-fired ceramics) technology they offer the advantage to use excellent conductors like silver, gold or mixtures of silver–palladium by co-firing at temperatures below 950 °C. The low sintering temperature is achieved by using a glass matrix, which has a low melting point and which allows liquid phase sintering of the glass ceramic composite material.[1] In most LTCC systems, the ceramic filler material, which is dispersed in the glass matrix is partially dissolved in the glass melt and starts to crystallise during the co-firing process. Since the development of dielectric LTCC base materials in the mid 1980′s[2–5] new types of green tapes, yielding different properties (e.g. medium dielectric constant,[6] low dielectric loss[7] or magnetic permeability[8]), have been added, and extended the range of applications. In the future, LTCC technology will play an important role in the development of microsystems with integrated electrical, magnetic, mechanical, thermal, chemical, biological and sensor functions,[9] which will lead to completely new devices in the near future.

As most of the LTCC papers, which are dealing with the properties of the glass-ceramics, investigate electrical or thermal behaviour, no publication is known to the authors, in which the lifetime prediction of LTCC was investigated due to its mechanical properties. This behaviour is of high interest, as in many applications the mechanical stress is an important issue regarding the reliability of the device. For automotive applications, robust mass flow sensors are needed for the ''on board'' diagnosis (OBD) of the injected fuel quantity from ''cycle to cycle'', to enhance the performance of modern Common-Rail (CR) injection systems and subsequently the combustion process. At a high-pressure hydraulic test bench, novel hot film anemometers, which were implemented into the body of injection nozzles for diesel passenger cars, were tested. The injection rate sensors consist of a LTCC-substrate (thickness: 840 μm, diameter ≈2.2 mm) with integrated electrical vias and

* Corresponding author. Tel.: +49-9131-852-7547; fax: +49-9131-852-8311.
E-mail address: roosen@ww.uni-erlangen.de (A. Roosen).

0955-2219/$ - see front matter © 2003 Elsevier Ltd. All rights reserved.
doi:10.1016/j.jeurceramsoc.2003.07.010

different thin film metallizations of molybdenum (Mo) or titanium/platinum (Ti/Pt) and demonstrated their functionality up to fuel injection pressures of 135 MPa (1350 bar).[10,11] For integrated devices, which have to operate under such chemically and mechanically harsh environmental conditions, it is of utmost importance to predict in advance the failure rate due to safety as well as cost aspects. To get reliable data of such small devices concerning mechanical failure, measurements of the mechanical properties had been performed using dimensions of the test specimens, which are comparable to the LTCC-substrate for the thermal mass flow sensors.

2. Experimental procedure

2.1. Specimen

The specimens were prepared from green tapes 951 (DuPont, USA). For this LTCC material a flexural strength of 320 MPa is given by the green tape manufacturer,[12] but the test conditions are not specified. Six blank green tapes 951 (DuPont, USA) had been punched to achieve the desired size, stacked and laminated without any vias and metallization by means of thermocompression. The green laminate was fired at 870 °C, following the binder burnout and firing schedule of the tape producer. The flat sintered laminate exhibited a thickness of 0.84 mm and a sintered density of $\rho = 3.1$ g·cm^{-3}. The LTCC ceramic was cut into pieces of two different sizes: 4.65×4.65 mm^2 and of 5.80×5.80 mm^2. The dicing of the ceramic plate was performed with a wafer saw.

2.2. Flexural strength measurement

For the determination of the flexural strength a ball-on-ring test was used.[13,14] The lower support had a diameter of 4 mm, the upper loading ball had a diameter of 5 mm. To determine the inert strength without any subcritical crack growth, a loading speed of 100 MPa/s was used (Universal Testing Machine, Model 4204, Instron Comp., High Wycom, USA). The flexural strength σ of 20 specimens from each size was determined from the load at failure and the stressed cross-section and thickness of the specimen. The results were plotted as a Weibull diagram,[13] which gives the characteristic strength σ_0 and the Weibull module m values. All calculations of the data had been performed following the ENV 843-5 standard.[15]

2.3. Crack growth rate v and parameters A and n

Using the ball-on-ring test described in Section 2.2., the flexural strength of the specimen had been determined at different loading speeds of 100, 10, 1 and 0.1 MPa/s. The results were also plotted as a Weibull diagram. These data give information of the influence of the loading speed on the strength behaviour. Information about this correlation have to be determined to calculate the lifetime prediction.

2.4. Life time prediction

To get information of the lifetime, a SPT (strength propability time) diagram must be set up. Therefore, the σ_0 and m values from the Weibull diagram and the parameters A and n of the subcritical crack growth are needed. The subcritical crack growth υ is given as

$$\upsilon = A \cdot K_{\mathrm{i}}^{n} \tag{1}$$

A, n: parameters of subcritical crack growth, K_{i}: stress intensity factor. To get A and n, the values of log σ_0 are plotted as a function of log $\mathrm{d}\sigma/\mathrm{d}t$ of the dynamic fatigue test. The dynamic fatigue is described by the following equation:

$$\sigma_B^{n+1} = B \cdot (n+1) \cdot \sigma_{\mathrm{in}}^{n-2} \cdot \mathrm{d}\sigma/\mathrm{d}t \tag{2}$$

$$\text{with} \quad B = 2/\left\{(n-2) \cdot A \cdot f^2 \cdot K_{\mathrm{ic}}^{n-2}\right\} \tag{3}$$

$$\text{and} \quad \sigma_{\mathrm{in}} = K_{\mathrm{ic}} \cdot \sqrt{a_{\mathrm{c}}} \cdot f \tag{4}$$

σ_{B}: fracture stress, σ_{in}: inert fracture strength, $\mathrm{d}\sigma/\mathrm{d}t$: loading speed, f: geometric factor (e.g. $f = \pi^{1/2}$ for an elliptical crack under tension in a plate of infinite size), K_{ic}: fracture toughness, a_{c}: critical crack length. From the slope of the curve and from the intercept of the axis, n and A are obtained. With these data the SPT diagram can be calculated, which allows to predict the life time of the measured samples. The failure probability as a function of time and stress is given by the following term:

$$\ln\ln 1/(1-P) = \left\{m/(n-2) \cdot \ln(t/t_{\mathrm{o}})\right\} \tag{5}$$

$$\text{with} \quad t_{\mathrm{o}} = 2/\left\{(n-2) \cdot A \cdot \sigma^n \cdot f^n \cdot \sqrt{a_{\mathrm{c}}^{n-2}}\right\} \tag{6}$$

P: failure probability of fracture, t: time to failure, m: Weibull modulus.

2.5. Young's Modulus

The Young's modulus E is determined via the measurement of the ultrasonic speed (USD 10, Krautkrämer, Hürth, Germany) at a frequency of 2 MHz. For these measurements LTCC specimen of 1.61 mm thickness of different size had been prepared via lamination of several stacked green tapes and subsequent firing under the same conditions like in case of the samples

with the size of 4.65 and 5.8 mm. The measurements were repeated several times at different specimen. The Young's modulus E is calculated from the following equation:

$$E = v^2 \cdot \rho \cdot (1 + \nu) \cdot (1 - 2\nu)/(1 - \nu) \quad (7)$$

v: speed of ultrasonic signal, ρ: density, ν: Poisson's ratio.

2.6. Analysis of crack origin

Ceramics are brittle materials, and therefore it is of high interest to get more information, where the crack has its origin in the microstructure. For this purpose, the microstructure of the specimen, which was broken with the loading speed of 0.1 and 100 MPa/s, was analysed in a optical microscope. After the detection of the position of the crack origin, the specimen were investigated in a scanning electron microscope (Stereoscan 250 MK3, Cambridge Instruments, Cambridge, UK) to detect the flaw in the microstructure, which was the reason for crack formation.

3. Results and discussion

3.1. Inert strength

The characteristic inert strength σ_0 for the two LTCC types including the Weibull module are given in Table 1. The corresponding Weibull diagram for the specimen of 4.65 mm size is shown in Fig. 1, which also indicates the confidential intervals for m and for the characteristic strength σ_0.

The characteristic flexural inert strength of the specimen with 5.8 mm length is 471.6 MPa (Weibull module m: 7.8). The confidential interval for the characteristic strength σ_0 is 448.1–496.0 MPa, and the confidential interval for m is 5.8–10.7. The specimen with only 4.65 mm length exhibits a lower characteristic inert strength of 439.6 MPa and a Weibull module of 8.2. The confidential interval for m is 6.1–11.2, and the confidential interval for the characteristic strength σ_0 is 418.8–461.2 MPa. The Weibull modules of both specimens are inside the confidential intervals for m, which means both specimen sizes follow the same defect distribution. The data sheet of DuPont for this tape 951 used[12] shows a flexural strength of non-metallised, fired LTCC-substrates of 320 MPa. A direct comparison is not possible, because there are no information in the data sheet concerning the used test method and type of specimen.

Contrary to all expectations the characteristic inert strength of the specimen with 5.8 mm length is higher than the strength of the smaller sample. During testing, the larger specimen reaches beyond the diameter of the lower support to a larger extend than the specimen of 4.65 mm size. This changes the stress distribution in the sample and results in a small increase of 7% in strength for the larger specimens. A FE-calculation would have been necessary to determine exactly the stress state and effective volume in the two specimen.

The data of the 4.65 mm specimens with a m-value of 8.2 show a good fit to the straight line of the Weibull diagram (Fig. 1). Above strength values of 330 MPa the data show a gap. Danzer et al.[16] could show that these gaps and peaks in the graph of the strength data of a small number of samples cannot be attributed to characteristic features of the material like bimodal strength distributions. But the low strength data of specimen are probably caused by large flaws in the microstructure, which are part of the flaw size distribution. This was

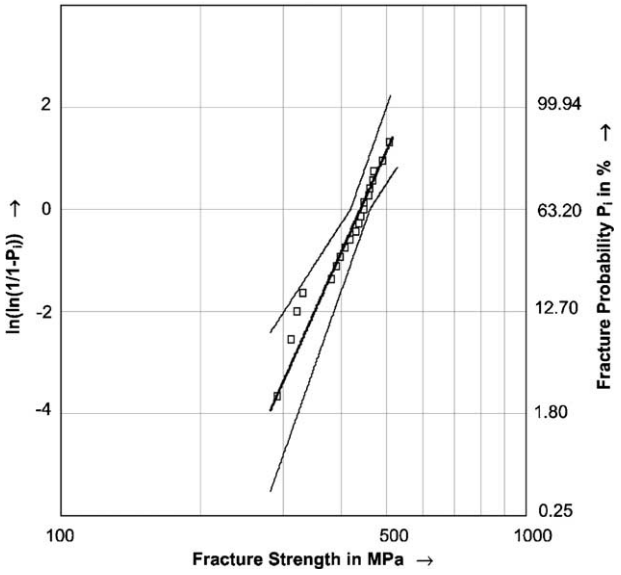

Fig. 1. Weibull diagram of the flexural strength data of LTCC specimen of 4.65 mm size with confidence interval, loading speed: 100 MPa/s.

Table 1
Characteristic inert strength and Weibull modulus of LTCC's

Specimen	Characteristic inert strength σ_0 [MPa]	Confidence interval of σ_0 [MPa]		Weibull module m [–]	Confidence interval of m	
		σ_l	σ_u		m_l	m_u
LTCC 5.8 mm	471.6	448.1	496.0	7.8	5.8	10.7
LTCC 4.65 mm	439.6	418.8	461.2	8.2	6.1	11.2

approved by the determination of the fracture origin by the analysis of the fractured samples. Fig. 2 shows e.g. a large pore of approximately 20 μm size, which was located at the surface of a sintered LTCC specimen and which was the origin of fracture.

3.2. Influence of loading speed on strength

3.2.1. Determination of σ_o and of Weibull module m

The characteristic strength σ_0, the Weibull module m, and their confidence intervals for the LTCC of 4.65 mm size in dependence on the loading speed had been calculated and are listed in Table 2. As expected, the strength of the specimens decreases with decreasing loading speed. A drop in strength from 440 to 310 MPa can be observed, the Weibull module is between 8.2 and 6.6.

3.2.2. Determination of Parameters A and n

To get A and n, the data log σ_0 and log $d\sigma/dt$ of the dynamic fatigue test are plotted (Fig. 3). The slope of the curve is $n=17.5$, the intercept of the curve with the axis is $A=3.86\cdot10^{-15}$. These values are typical values for oxide ceramics like Al_2O_3.

3.3. Life time prediction

From the Weibull diagram of the inert strength (Fig. 1), the slope $m=8.2$ and $\sigma_0=439.6$ MPa were obtained. Using these data as well as $n=17.5$ and $A=3.86\cdot10^{-15}$, the SPT diagram can be calculated (Fig. 4), which allows to predict the life time of the measured parts.

Fig. 4 informs about the failure probability for specific life times at given stresses. E.g., at an applied stress σ of 80 MPa, the fracture propability F is 1.8%, which means 1.8% of the specimens are broken after a time t of 10 years. The deviation of the strength data also influences the deviation of the predicted life time. This is the reason why already some specimen failure at low stresses. Until all parts are broken, it takes a long time, e.g. more than 50 years, if the parts are stressed with a load of 100 MPa. It was shown that the size of the specimen influence the value of the inert strength. But the larger characteristic inert strength of the larger specimen has only a minor influence on the SPT diagram.

3.4. Young's modulus

The density of the sintered LTCC material had been determined as 3.1 g/cm^3, the Poissońs ratio of $\nu=0{,}17$ was given in the data sheet.[17] For the measured average ultrasonic signal speed of $v=5286$ m/s, the Young's modulus was determined as $E=153$ GPa. This value is nearly identical with the value of 152 GPa, which is

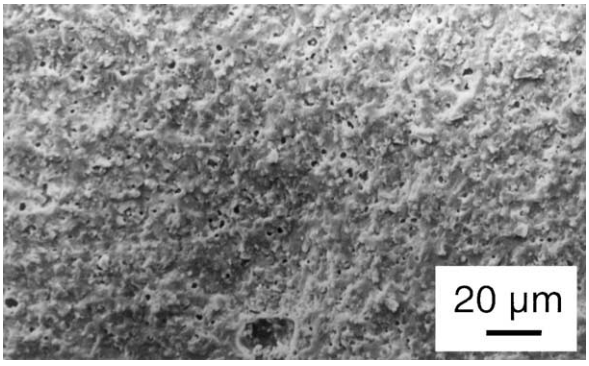

Fig. 2. Scanning electron micrograph of a fractured LTCC sample of low strength with a crack origin at a large pore.

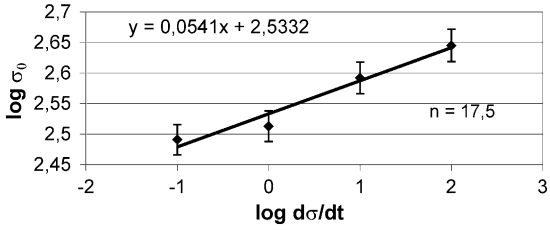

Fig. 3. Dynamic fatigue test of LTCC specimen of 4.65 mm size.

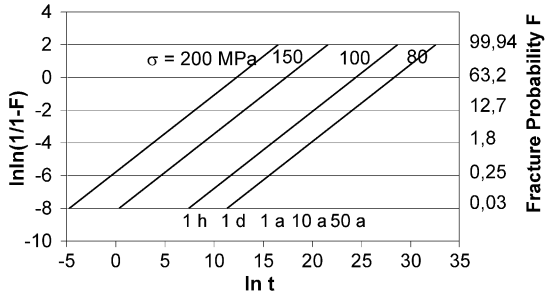

Fig. 4. Lifetime prediction diagram for LTCC specimen.

Table 2
Characteristic strength and Weibull modulus of LTCC's in dependence on loading speed (size of the specimens: 4.65 mm)

$d\sigma/dt$ [MPa/s]	Characteristic strength σ_0 [MPa]	Confidence interval of σ_0 [MPa]		Weibull module [–]	Confidence interval of m	
		σ_l	σ_u		m_l	m_u
100	439.6	418.8	461.2	8.2	6.1	11.2
10	391.1	368.0	415.2	6.6	4.9	8.9
1	326.3	309.1	344.2	7.4	5.5	10.1
0,1	310.1	291.8	329.2	6.6	4.9	9.0

Table 3
Analysis of crack origin

Crack Origin	Large pore close to surface	Crack at surface	Large grain close to surface	Not identified
Number	8	4	2	6

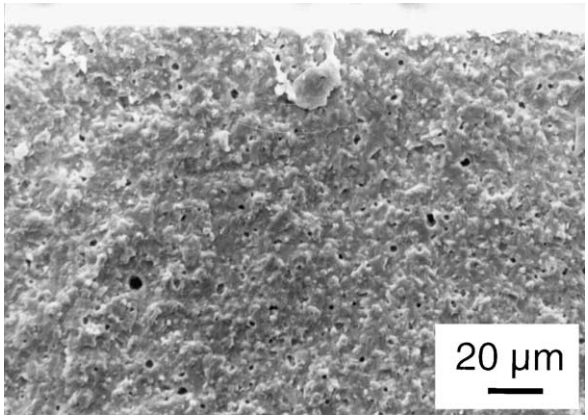

Fig. 5. Scanning electron micrograph of a fractured LTCC sample showing a crack origin at a large grain located close to the surface.

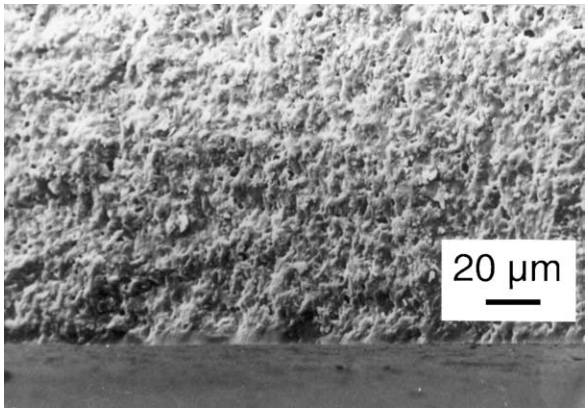

Fig. 6. Scanning electron micrograph of a fractured LTCC sample showing a crack origin at a glass-rich region located close to the surface.

given in the data sheet. Again, no information is given by DuPont, how this value was determined.

3.5. Analysis of crack origin

By microstructure analysis of the broken specimen it is possible to ascribe failure to specific defects. For 14 of 20 samples the crack origin could be localised (Table 3). In most cases the crack started from defects, which were located close to the surface, and a larger pore was the origin of the crack of failure (see Fig. 2). Less often cracks and large grains (Fig. 5) had been the reason for failure. In some cases the crack started from regions of higher glass amount (Fig. 6). A clear decision whether the failure starts e.g. from a crack or a larger pore is not always possible. Large pores with radii up to 20 µm are the most common cause for failure.

4. Conclusions

The characteristic inert flexural strength of the investigated LTCC material is in the range of 439.6–471.6 MPa. Due to the used ball-on-ring test the strength shows a higher level than in case of using the ring-on-ring test. The LTCC producer declares a value of 320 MPa, but no reference is given for the used test method.

In applications with a stress level of 100 MPa acceptable lifetimes are achieved. Mass flow sensors for the measurement of the injected fuel quantity in the high-pressure hydraulic system of Common-Rail (CR) injection systems are exposed to such stress levels. These sensors are needed for the ''on board'' diagnosis (OBD) to enhance the performance of modern CR injection systems and subsequently of the entire automotive combustion process. They are implemented into the body of injection nozzles for diesel passenger cars.

It was shown that the size of the specimen relative to the size of the ball-on-ring set-up had an influence on the mechanical properties. The measurements had been done using the same ball-on-ring set-up for the two series of specimen, which only differ in their size. Because the smaller specimen did not protrude the ring of the ball-on-ring set-up, unspecified peaks of stress can occur in the edge region of the sample, thus the smaller specimens exhibited the lower strength level (439.6 MPa) than the larger specimens (471.6 MPa). In case of an adapted ball-on-ring geometry, the smaller specimens should exhibit the higher strength level, due to the lower stressed volume, which results in statistically less defects in the volume of the specimen. A FE-calculation would be helpful to investigate the stress state and the effective volume of the two square shaped samples.

The strength level of LTCC is lower than the strength level of alumina under comparable test conditions, but the strength is sufficient for many applications, in which the device is mechanically stressed. For this reason LTCC is an interesting base material to fabricate devices, in which LTCC fulfils the requirements of a functional and also structural material. The level of strength could be improved, if the tape producer would eliminate larger pores and other inhomogeneities in the green tape.

Acknowledgements

The authors would like to thank Professor Dr. R. Weißmann from the Institute of Materials Science for fruitful discussions concerning the evaluation of the strength data.

References

1. Ewsuk, K. G., Ceramic-filled-glass composite sintering. *Ceramic Transactions*, 1990, **15**, 279–295.
2. Kata, K., Shimada, Y. and Takamizawa, H., Low dielectric constant new materials for multilayer ceramic substrate. *IEEE Trans. Compon., Hybrids, Manuf. Techn.*, 1990, **13**, 448–451.
3. Tummala, R. R., Ceramic and glass-ceramic packaging in the 1990s. *J. Am. Ceram. Soc.*, 1991, **74**, 895–908.
4. Knickerbocker, J. U., Overview of the glass-ceramic/copper substrate—a high-performance multilayer package for the 1990s. *Am. Ceram. Soc. Bull.*, 1992, **72**, 1393–1401.
5. Knickerbocker, S. H., Kumar, A. H. and Herron, L. W., Cordierite glass-ceramics for multilayer ceramic packaging. *Am. Ceram. Soc. Bull.*, 1993, **72**, 90–95.
6. Dernovsek, O., Naeini, A., Preu, G., Wersing, W., Eberstein, M. and Schiller, W. A., LTCC glass-ceramic composites for microwave application. *J. Eur. Ceram. Soc.*, 2001, **21**, 1693–1697.
7. Amey, D. I., Keating, M. Y., Smith, M. A., Horowitz, S. J., Doahue, P. C. and Needs, C. R., Low loss tape materials system for 10–40 GHz application. *Proc. Intern. Symp. on Microelectronics, Boston, MA, Sept.*, 2000, 654–658.
8. Feingold, A.H., Heinz, M. and Wahlers, R.L., Compliant dielectric and magnetic materials for buried components. *Proc. Intern. Symp. on Microelectronics, Denver, CO, Sept.* 2002, 65–70.
9. Wilcox, D.L., Multilayer ceramic microsystems technology—an overview, *Proc. European Microelectronic and Packaging Conf. 2001, IMAPS France, Versailles*, 2001, 115–117.
10. Schmid, U., A robust flow sensor for high pressure automotive applications. *Sensors and Actuators A: Physical*, 2002, **97-98**(C), 253–263.
11. Schmid, U., Krötz, G. and Schmitt-Landsiedel, D., Injection rate measurements with robust thin film sensors. *Proc. XVI EUROSENSORS in Prague*, 2002, 391–392.
12. DuPont Photopolymer & Electronic Materials: 951 Low-Temperature Co-fired Dielectric Tape, UK, 1998.
13. Munz, D. and Fett, T., *Ceramics: Mechanical Properties, Failure Behaviour, Materials Selection*. Springer-Verlag, Berlin Heidelberg, 2001.
14. Shetty, D. K., Rosenfield, A. R., McGuire, P., Bansal, G. K. and Duckworth, W. H., Biaxial flexural tests for ceramics. *Am. Ceram. Soc. Bull.*, 1980, **59**, 1193–1197.
15. ENV 843-5: Advanced Technical Ceramic, Mechanical Properties at Room Temperature, Part 5: Statistical Analysis, 1996.
16. Danzer, R., Lube, T. and Supancic, P., Monte Carlo simulations of strength distributions of brittle materials. *Z. Metallkunde*, 2001, **92**, 773–783.
17. DuPont Photopolymer & Electronic Materials: Tape Overview, EKP, UK, 1999.